Journal of Engineering Issues and Solutions

Seismic fragility assessment of low-rise reinforced concrete frame: A comparative study of bare and infill model

Rajan Suwal[1,*], Rupesh Uprety[1]

[1]*Department of Civil Engineering, Pulchowk Campus, Institute of Engineering, Tribhuvan University, Nepal*
**Corresponding email: rajan_suwal@ioe.edu.np*

Received: November 10, 2022; Revised: February 18, 2023; Accepted: March 06, 2023

doi:https://doi.org/10.3126/joeis.v2i1.49373

Abstract

Most of the residential structures designed in Nepal are low-rise reinforced concrete (RC) frames. They are designed following the guidelines given in the Nepal Building Code, especially, the mandatory rule of thumb. In analyzing and designing most of the reinforced concrete structures in the urban and semi urban areas of Nepal, only bare frame model is considered. The additional effect caused by the infill walls are neglected. In this research, a comparative seismic fragility assessment of low-rise RC frame is conducted. Two cases are assumed; with and without the consideration of the unreinforced masonry infill. Macro modelling approach is followed for modelling the infill effect. Results clearly indicate that the inclusion of the infills drastically reduce the roof displacement compared to the bare frame model during a seismic shaking. This is attributed to the fact that the inclusion of the infill imparts more stiffness to the structure during a seismic-shaking compared to the bare frame model and hence the displacement is reduced. Furthermore, seismic fragility of the frame structure is also overstated when the effect of infill is not taken into consideration. The inclusion of infills reduced the structural fragility to significant extent. In this regard, the bare frame model was found to be more vulnerable to seismic shaking compared to the infill model.

Keywords: *Distributed plasticity, Fragility, Infills, Macro-modelling, OpenSees*

1. Introduction

It is a common practice to use masonry infill walls as a partition wall in many countries, especially for the low-rise reinforced concrete (RC) frames. It is also, at the same time, a common practice to neglect the effect brought about by the masonry infill walls during an earthquake-shaking. Infills can contribute to a significant amount in increasing the lateral stiffness of a structure. Pujol and Fick (2010) performed experimental studies on the effect caused by masonry wall on the seismic performance of structures. Teguh (2017) performed experimental studies on the masonry wall subjected to cyclic loading and concluded that including masonry infill provide alternate load path on a frame system and thus highlighted its importance. This study further concluded that the infill walls can be beneficial during a structural response provided that

they are placed regularly throughout the structure and they do not cause the shear failure of the tie columns. Shan et al. (2016) performed experimental studies on the progressive collapse performance of RC frames with infill walls. To this end, a two-storey RC frame was analyzed experimentally as well as in OpenSees (McKenna and Fenves, 2000) with and without the inclusion of infills. They concluded that the inclusion of infills impart stiffness to the structure at the cost of a reduced ductility. The presence of infill walls can be beneficial or unfavorable on structures (Furtado et. al, 2015). The negative impacts are associated with the horizontal and vertical irregularities brought about by the masonry infills that can cause various failure mechanisms in structures like the soft storey mechanism (Furtado et. al, 2014) and short column mechanism (Dolsek and Fajfar, 2008). Out-of-plane collapse of infill walls is one of the most dangerous failure modes that possess great risk to occupants (Furtado et al., 2015). Barbosa et al. (2017) studied the performance of mid to high rise RC frame buildings with masonry infills during 2015 Gorkha earthquake. Kose (2009) carried out extensive research to study the parameters affecting the fundamental period of the RC frames with infills. The selection parameters were building height, number of bays, ratio of area of shear wall to area of floor, ratio of infill panels to total number of panels and type of frames. He concluded that RC frames with infills have shorter period (5%-10%) regardless of whether the shear wall is present or not.

Furtado et al. (2015) studied the influence of the in plane and out-of-plane walls' interaction on the structural response of RC frames. The study proposed a simplified macro model which accounts for the out-of-plane behavior of infill walls as well as the interaction of in plane and out-of-plane behavior during seismic shaking. Asteris et al. (2017) also performed studies on the out of plane behavior of the infill walls. Asteris et al. (2015) have proposed a macro-modelling approach to model the masonry infill walls by considering the openings and vertical loads. Asteris et al. (2016) studied on calculation of the fundamental period of RC frames with infills. They performed a research work to predict the fundamental mode period of a RC frame structure with infills using artificial neural network. Uprety and Suwal (2023) performed bidirectional analysis of low-rise bare and infill frames and conducted seismic fragility assessment of the same. The result of the analysis clearly depicted that the performance of the structures was significantly impacted when the infills' effect was taken into consideration. Bare frame models were found to be more fragile compared to the infill ones, thus highlighting the importance of modelling infills during a seismic shaking. Fikri and Ingham (2022) performed analysis to develop seismic response and aftershock fragility curves for a non-ductile mid-rise RC frame with infill. These non-ductile mid-rise masonry infill buildings were seismically assessed using incremental dynamic analysis (IDA) and a series of aftershock fragility curves for various damage states following mainshock shaking were produced. It was discovered that when a building's Inter-storey Drift Ratio (IDR) grew, aftershock shaking caused more damage at a lower spectral acceleration intensity, demonstrating that these mainshock-damaged structures were extremely vulnerable to earthquakes of lower aftershock intensity. Adhikari et al. (2022) performed the seismic fragility assessment of low-rise RC frames with brick infills in high seismic regions. For a single model, different cases were considered; bare frame model with soil structure interaction, infill model with soil structure interaction, bare frame model without soil structure interaction and infill model without soil structure interaction. The overall picture of the observations showed that low-rise RC buildings were damage state sensitive to the effects of infills and soil-structure interaction. In the meanwhile, because some performance criteria are more sensitive than the total fragility, design considerations would be severely impacted. In the case of low-rise RC buildings, it was also noticed that the analytical fragility models significantly overstated the real seismic fragility.

The importance of infills in modelling of RC frames have been extensively highlighted, however it is still in practice, in case of Nepal, to ignore its effect during a seismic shaking. Extensive researches have been done to highlight the importance of infills and the modelling of infills, yet very little work has been done in this area. Hence, in order to bridge the research gap, a low-rise RC frame model was selected for this research

work. Major objective of this research is to study the seismic performance of bare and infill model in case of an earthquake event. Time history analysis was done for this case. Global behavior was studied and roof displacement was taken as the global variable. Secondly, fragility analysis was performed for both bare and infill model and fragility curves were prepared, compared and contrasted.

2. Material and Methods

2.1. Prototype building model

A three-storey RC frame was considered for this study. The model was prepared in OpenSees (McKenna and Fenves, 2000). Two instances of model were prepared in OpenSees as shown in **Figure 1**. First one was the bare frame case, where the effect of infill was not considered. In the second case, the infill effect was considered for the exterior walls. The model considered had 3 numbers of bay in x and y direction. Fixed based model was considered and the soil structure interaction was not considered. The finite element model parameters and geometric properties of the structure is listed in **Table 1** and **Table 2.** The reinforcement details of the model are listed in **Table 3**. The typical cross section of beam and column is shown in **Figure 2.**

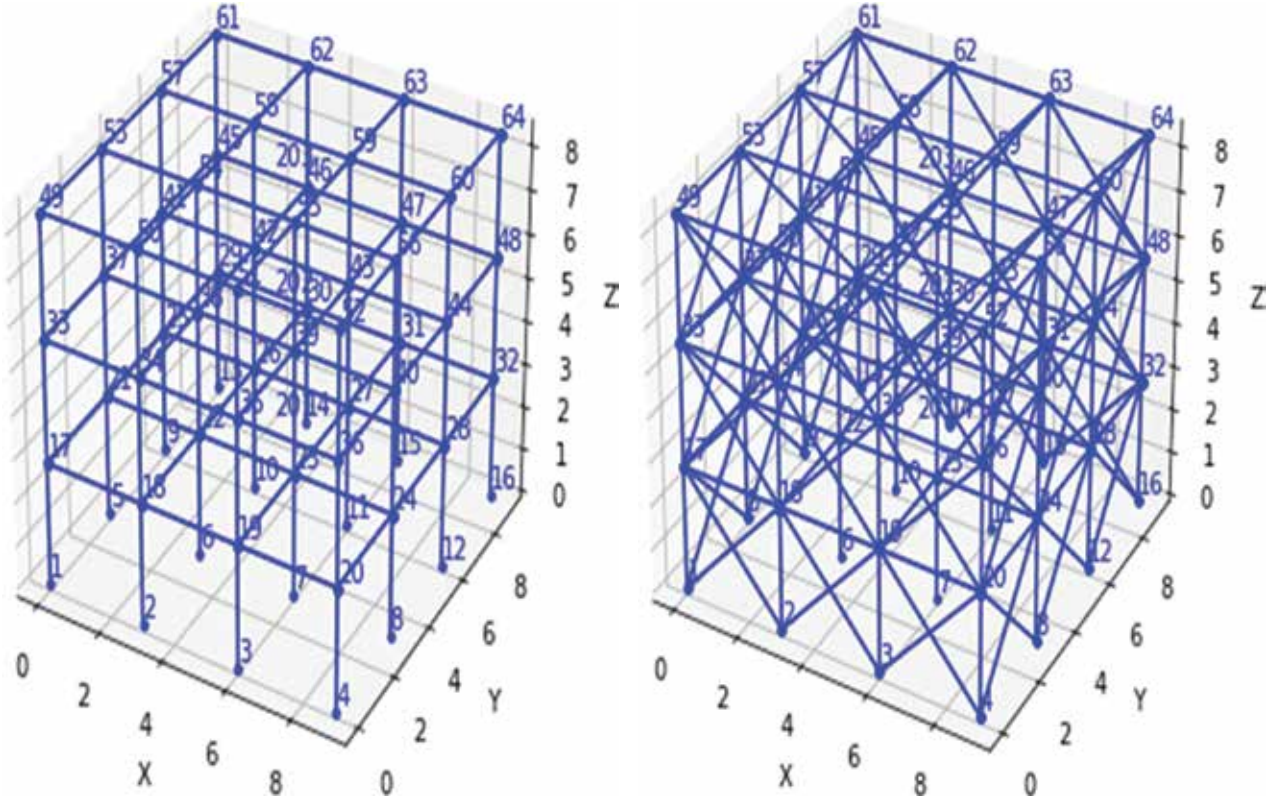

Bare Frame Case Infill Case

Figure 1: Finite element models considered for the study purpose

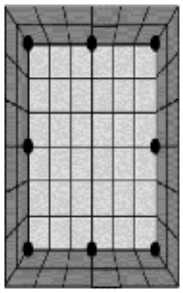

Core Concrete = 6x6 no. of fibers

Cover Concrete = 6x2/2x6 no. of fibers

Column Section

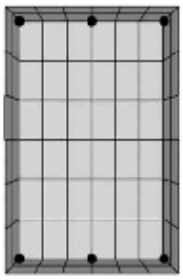

Core Concrete = 6x6 no. of fibers

Cover Concrete = 6x2/2x6 no. of fibers

Beam Section

Figure 2: Cross section of beam and column

Table 1: Structural properties of model parameters

Model Case	Bare	Infill
Beam Size	230x350 mm	230x350 mm
Column Size	300x300 mm	300x300mm
Slab Thickness	127 mm	127 mm
Bay No	3x3	3x3
Bay Length	3m x 3m	3m x 3m
Live Load	1 kN/m^2	1 kN/m^2
Floor Finish	0.5 kN/m^2	0.5 kN/m^2

Table 2: Finite element model parameters

Parameters	**Value**	**Units**
Yield Strength of Steel (f_y)	415	MPa
Ultimate Strength of Steel (f_u)	485	MPa
Yield Strain of Steel (ϵ_y)	0.002075	-
Ultimate Strain of Steel (ϵ_u)	0.144	-
Modulus of Elasticity of Steel (E_s)	2×10^5	MPa
Modulus of Elasticity of Concrete =$5000\sqrt{fck}$	22360.68	MPa
Poisson's Ratio for Concrete (υ)	0.2	-
Shear Modulus = E/2(1+υ)	9316.95	MPa
Unit Weight of Concrete	25	kN/m^3
Concrete Strain at Maximum Stress in Axial Compression (IS 456:2000; Clause 39.1)	0.002	-
Concrete Strain at Maximum Stress in Axial Compression and Bending (IS 456:2000; Clause 39.1)	0.0035	-

Table 3: Beam and column specification

Floor Level	Longitudinal Rebar of Beam	Longitudinal Rebar of Column	Lateral Ties for Column	Shear Reinforcement for Beam
Second Floor	3 @ 12mm –Top 3 @ 12mm- Bot.	8@ 12mm Φ	8mm Φ-125mm c/c	2LVS, 8mm Φ-100mm c/c
First Floor	3 @ 12mm –Top 3 @ 12mm- Bot.	8@ 12mm Φ	8mm Φ-125mm c/c	2LVS, 8mm Φ-100mm c/c
Ground Floor	3 @ 16mm –Top 3 @ 16mm- Bot.	8@ 16mm Φ	8mm Φ-125mm c/c	2LVS, 8mm Φ-100mm c/c

Note: Bot. = Bottom Rebar; Top = Top Rebar; c/c = center to center spacing; 2LVS = 2 Leg Vertical stirrup

2.2. Modelling of masonry infill

Infill walls can be of different types; namely brick, stone, cement block and so on. All of these are in common practice in context of Nepal. However, in the urban and semi-urban regions of Nepal, brick infills are extensively used. Hence, in this study we have considered the brick infill. Different approaches of modelling the brick infill masonry panel is available in the literature. On a broader scenario, they can be classified into two groups, namely micro-modelling approach and simplified macro-modelling approach. In the micro-modelling approach, the effect of mortar joints is also considered. Mortars joints are actually the weakest points of failure in masonry infill and hence the micro-modelling approach can best represent the seismic performance and behavior of a masonry wall. Micro-modelling approach requires different components of a masonry system to be properly defined such as the bricks, mortar, interface brick-mortar, interface masonry-frame, and the frame elements. Due to the complex modelling adopted by this approach, it is computationally expensive and is generally not followed to study the global performance of a structure. Micro-modelling approach can be best suited when studying the local behavior of the masonry walls. Macro-modelling, on the other hand, requires that the infill effect in a frame structure be modelled using an equivalent compressive diagonal strut. In general, single compressive struts are defined in two diagonal directions to represent the infill masonry. There are other approaches also available in the literature to model the infills using the diagonal struts (Rodrigues et al., 2010). In case of macro modelling, equivalent width of a diagonal strut is calculated. FEMA (2003) and IS code follows similar approach for calculation of the width of the diagonal struts. Macro modelling approach has been adopted in our case.

Another major step in macro-modelling approach for nonlinear analysis is the definition of the constitutive relation that is to be assigned to the diagonal compression strut. This will represent the post elastic behavior of the diagonal strut during seismic shaking. Different researchers have provided varieties of constitutive relation for modelling the force deformation relationship of the diagonal compression strut. Fardis (1996) and Dolsek and Fajfar (2008) are two of the mostly used approaches currently established in the literature to describe the nonlinear response of masonry infill. The approach provided by Fardis (1996) was adopted for defining the nonlinear force deformation behavior of the diagonal strut. It is a multi-linear curve, characterized by four stress states: initial elastic behavior of the infill at un-cracked stage, post-elastic linear response characterized by a reduced value of stiffness, softening response after the maximum force and residual strength state as shown in **Figure 3.** Several parameters are needed to define the backbone curve

given by Fardis (1996). The initial stiffness R1 of the masonry was calculated as

$$R1 = \frac{G_m t_m L_m}{H_m} \quad (1)$$

where, G_m is shear modulus of the infill obtained from diagonal compression test and L_m, t_m and H_m are the length, thickness and height of masonry infill panel respectively.

The post cracking stiffness R2 can be calculated using the following expression:

$$R2 = \frac{E_m t_m b_m}{d_m} \quad (2)$$

where, E_m is the Young's modulus of elasticity of masonry wall, d_m is the diagonal length of the masonry infill and b_m is the thickness of the strut as calculated in **Equation 5**.

Similarly, R3 is the stiffness of the softening branch which was taken as 0.5% to 10% of the initial branch R1.

The lateral cracking strength F_y is calculated as:

$$F_y = f_{ms}\, t_m\, l_m \quad (3)$$

where, f_{ms} is cracking stress of the masonry wall as measured in diagonal compression test. The ultimate strength F_u was taken as:

$$F_u = 1.3 f_{ms}\, t_m\, l_m \quad (4)$$

Residual strength F_R can be taken as 5-10% of the ultimate strength of the masonry infill.

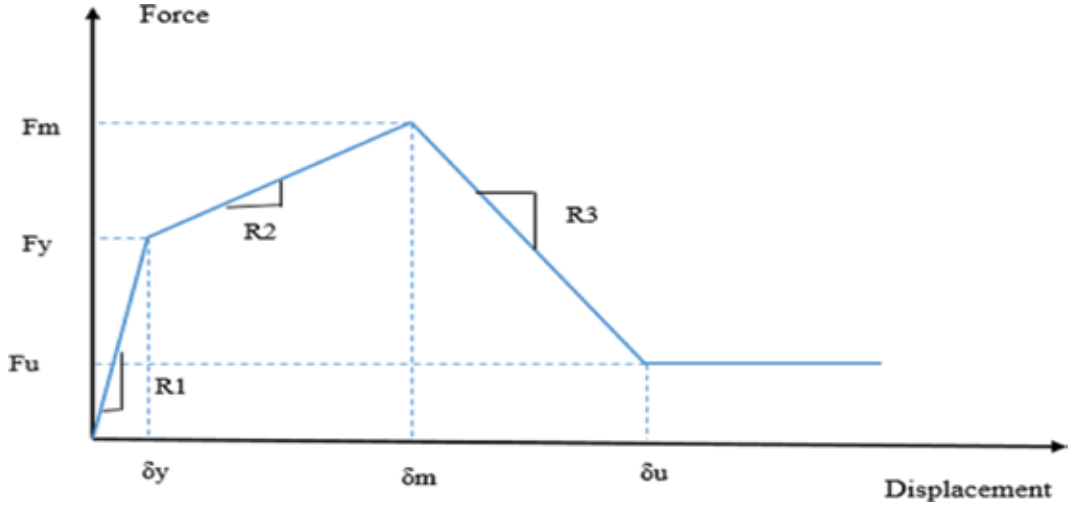

Figure 3: In plane lateral constitutive model proposed by (Fardis, 1996)

For calculation of the strut width, the equation recommended by FEMA (2003) was adopted. The equivalent width was calculated using following expression:

$$b_m = 0.175\,(\lambda_1 h_{col})^{-0.4} r_{inf} \quad (5)$$

where $r_{inf} = d_m$ is the diagonal length of the infill wall and λ_1 is calculated as :

$$\lambda_1 = \left[\frac{E_m\ t_m \sin 2\theta)}{4\ E_{fe}\ I_{col}\ h_{inf}}\right]^{1/4} \quad (6)$$

where, E_{fe} is the modulus of elasticity of the frame, I_{col} is the moment of inertia of the column and $h_{inf} = h_m$ is the height of masonry infill. The material properties of masonry infill are taken form Varum (2003) based on the diagonal compressive test results of masonry wallets with plaster on both sides. Modulus of elasticity, tensile strength, and shear modulus are respectively taken as 2300 MPa, 0.575 MPa and 1.171 GPa respectively. The infill effects brought about by the interior half walls are not considered and only their seismic effects are considered. The value of Fy, Fm, and Fu were respectively 357.075kN, 464.198kN, 46.4198 kN and ⍰y, ⍰m, and ⍰u of 1.2mm, 3.083mm, and 17.158mm respectively.

2.3. Ground motion selection

One of the major aspects of nonlinear time history analysis is the selection of earthquake ground motion. The seismic performance of structures is highly dependent upon the ground motion characteristics. A total of 14 earthquake ground motion records were taken into consideration for this study purpose. The ground motions were selected such that they represented a variation in their magnitude, frequency content, and duration. The selected ground motions for this analysis purpose is shown in **Table 4**. The ground motion records were downloaded from the NGAwest2 records (Ancheta et al., 2013) available in the PEER Strong Ground Motion Database (PEER, 2005) except the Gorkha earthquake, which is downloaded from strong motion center. The selected ground motions were a combination of near field and far field shaking. These selected ground motions were then used to perform time history analysis and the responses are recorded and studied.

Table 4: List of selected earthquakes

S.N.	Earthquake Name	Year	Station	Mw	Hyp (km)	H1(g)
1	Gorkha	2015	Kantipath	7.8	78.2	0.164
2	Kocaeli, Turkey	1999	Yarimca	7.51	25.07	0.322
3	Kobe, Japan	1995	Kobe University	6.9	31.08	0.312
4	Chalfant Valley-02	1986	Tinemaha Res. Free Field	6.19	57.99	0.447
5	Loma Prieta	1989	BRAN	6.93	19.66	0.502
6	Imperial Valley-06	1979	Bonds Corner	6.53	11.72	0.777
7	Coalinga-05	1983	Oil City	5.77	8.71	0.841
8	Northridge	1994	J. F. Plant Generator Building	6.69	21.08	0.995
9	Coyote lake	1979	Gilroy Array #6	5.74	9.12	0.422
10	N. Palm Springs	1986	Whitewater Trout Farm	6.06	11.79	0.629
11	Umbria Marche, Italy	1997	Nocera Umbra	6.0	12.49	0.472
12	Whitter Narrows-01	1987	Whittier Narrows Dam upstream	5.99	15.18	0.317
13	San Fernando	1971	Pacoima Dam (upper left abut)	6.61	17.6	1.238
14	Managua, Nicaragua-01	1972	Managua, ESSO	6.24	7.57	0.372

2.4. Nonlinear modelling

Nonlinearity in a structure are of different types, namely, geometric nonlinearity, material nonlinearity and contact nonlinearity. For our case, we only considered the material nonlinearity while performing the nonlinear time history analysis. Again, there are different approaches of modelling the material nonlinearity in a structure. They are distributed plasticity approach and concentrated plasticity approach. In the concentrated plasticity approach, nonlinearity is lumped at specific locations, usually at the ends of elements and the elements is modeled as linear. Unlike this, the distributed plasticity approach assumes that nonlinearity can occur anywhere within the elements and assumes the entire element as nonlinear. It then assigns suitable integration points to the elements and adopts suitable integration scheme for carrying out the analysis. Distributed plasticity approach is adopted for this analysis. Nonlinear beam column element, which is an OpenSees implementation of force-based element, is used to model the beams and columns. The nonlinearity is lumped at six integration points per elements. A wide range of numerical integration options are available in OpenSees to represent distribute plasticity in force-based beam-column elements (Scott, 2007). Gauss-Lobatto type of integration was used in our case in nonlinear beam column element. This is a most common type of integration scheme adopted for force-based element (Neuenhofer & Filippou, 1997). Gauss Lobatto type integration assigns integration points at the ends of an element section as well where the bending moments are maximum (Scott, 2007). In addition to the material nonlinearity, geometric nonlinearity (P-Δ effect) has not been considered in the analysis.

In OpenSees, fiber sections were created for beams and columns. Nonlinear beam column element was used to model the beams and columns. Concrete02 and Steel02 (Carreo et al., 2020) was respectively used to represent the nonlinear material behavior of the concrete and steel reinforcements. For concrete, the effect brought about by the confinement was also taken into consideration for the confine concrete (Mander et al., 1989). Concrete fibers were created for confine and unconfined concrete. **Figure 4** shows the stress-strain behavior for the Concrete02 and Steeel02.

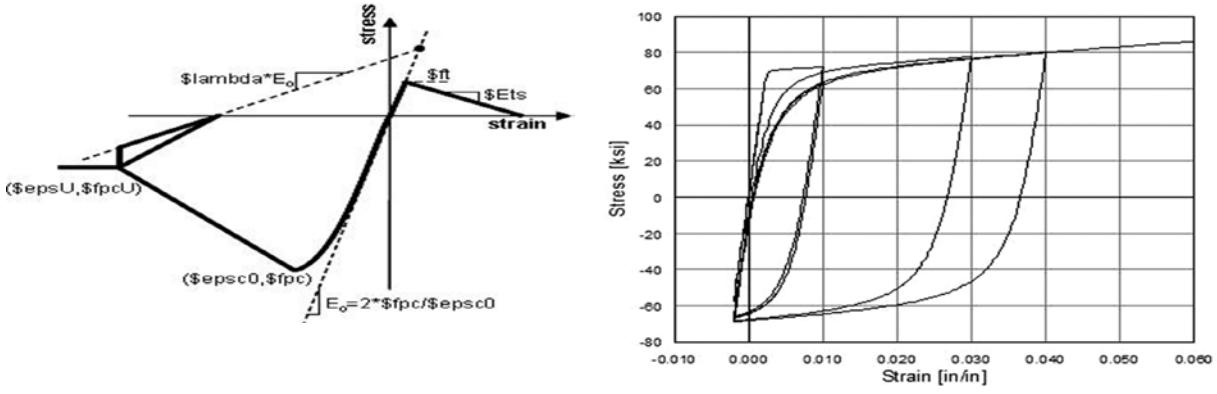

Figure 4: Hysteretic behavior of Concrete02 (left) and Steel02 (right) (McKenna and Fenves, 2000)

In case of the diagonal strut, it was modelled using the truss element in OpenSees. Hysteretic Material model was adopted to represent the cyclic behavior of the compression strut. In order to define the cyclic behavior using Hysteretic Material model, three points in tension and compression are required. Small values (1% of that of the compression) was provided in the tension zone to simulate no tension response and, at the same time, maintain the numerical stability. Mohammad Noh et al. (2017) have performed the validation of the experimental and OpenSees model considering infill and performed model calibration, when using the Hysteretic Material model. The model parameters that include pinchx, pinchy and beta values were hence adopted from their calibration.

2.5. Fragility analysis

Fragility functions define the probability of exceedance of certain damage state for a structure for a particular level of seismic demand. The seismic demand are the intensity measures which can be peak ground acceleration, peak ground velocity, peak ground displacement or the spectral acceleration. There is different approach of deriving fragility functions. They are expert based/ judgmental fragility curve, experimental fragility curve, empirical fragility curve and analytical fragility curve. In the absence of sufficient expert judgments or field data, analytical fragility curves are generated. Analytical method was adopted in this paper to define the fragility function. Four types of damage states were considered while preparing the fragility curve. They were slight, moderate, extensive and complete damage states. The famous and widely used limit state model proposed by Lagomarsino and Giovinazzi (2006) is used to define the median limit states for four damage states.

Slight damage = 0.7 d_y (7)

Moderate damage = 1.5 d_y (8)

Extensive damage = 0.5(d_u + d_y) (9)

Complete damage = d_u (10)

Idealization of the capacity curve gives the yield (d_y) and ultimate displacements (d_u). The median values of the four-damage state were calculated using the equations 7-10 by using the yield and ultimate displacement values calculated by performing the bilinear idealization of capacity curve.

$$P[\frac{ds}{S_d}] = \emptyset[\frac{1}{\beta_{ds}} \ln(\frac{Sd}{S_{d,ds}})] \quad (11)$$

Where, $\emptyset$ = the standard normal cumulative displacement function,

$S_{d,ds}$ = median values at which the building reaches the threshold of damage state, *ds*.

$S_{d,ds}$ is calculated from equations 7-10 and

β_ds = the standard deviation of the natural logarithm of the engineering demand parameters (EDP) for damage states, *ds*.

3. Results and Discussion

3.1. Modal validation

Validation of OpenSees model is an important step before moving on to any further analysis. At first, the bare frame models built in OpenSees were validated by performing the modal analysis (Chopra, 2001). The modal properties that include the modal period, frequencies and mode shapes were checked and compared. Modal period for the first three modes of the bare frame model was compared with the values obtained from the ETABS V.19 software. **Table 5** shows the values of modal period for the first three modes which are in good agreement and justified. Comparable values of modal periods were obtained in ETABS and OpenSees with slight discrepancy which confirmed the correctness of our numerical model that we prepared in OpenSees. Once the bare frame models were validated, then only the infill effects were applied to the frames.

Table 5: Modal period

Analysis Tool	ETABS	OpenSees
Mode 1	0.352 s	0.366 s
Mode 2	0.352 s	0.366 s
Mode 3	0.306 s	0.274 s

3.2. Roof displacement

Roof displacement was considered as the global parameter to be studied in this analysis. **Table 6** shows the roof displacement obtained for the bare and infill model for all the selected earthquake ground motions. Addition of infill caused a drastic reduction in the roof displacement in model. The infills provided additional stiffness to the model as compared to the bare frame model. This depicted the significance of infills in the analysis and highlighted its modelling importance as well.

Table 6: Roof displacement in mm

Model Type		M1 Model	
S.N.	Earthquakes	Bare	Infill
1	Gorkha	32.44	2.845
2	Kocaeli, Turkey	44.7	3.547
3	Kobe, Japan	33.675	3.395
4	Chalfant Valley-02	72.671	4.881
5	Loma Prieta	85.083	6.029
6	Imperial Valley-06	99.605	7.613
7	Coalinga-05	86.348	7.366
8	Northridge	109.713	8.25
9	Coyote lake	53.589	3.973
10	N. Palm Springs	65.968	5.44
11	Umbria Marche, Italy	40.821	5.069
12	Whitter Narrows-01	29.395	5.017
13	San Fernando	110.118	11.066
14	Managua, Nicaragua-01	51.54	4.475

3.3. Fragility curves

Time History analysis was performed on a typical low-rise RC frame for the selected 14 sets of ground motion. Analytical fragility curves were than prepared for the two cases to compare and contrast the structure vulnerability with and without the consideration of the unreinforced masonry infills. The structural fragility for both bare and infill case is represented in **Figure 5**.

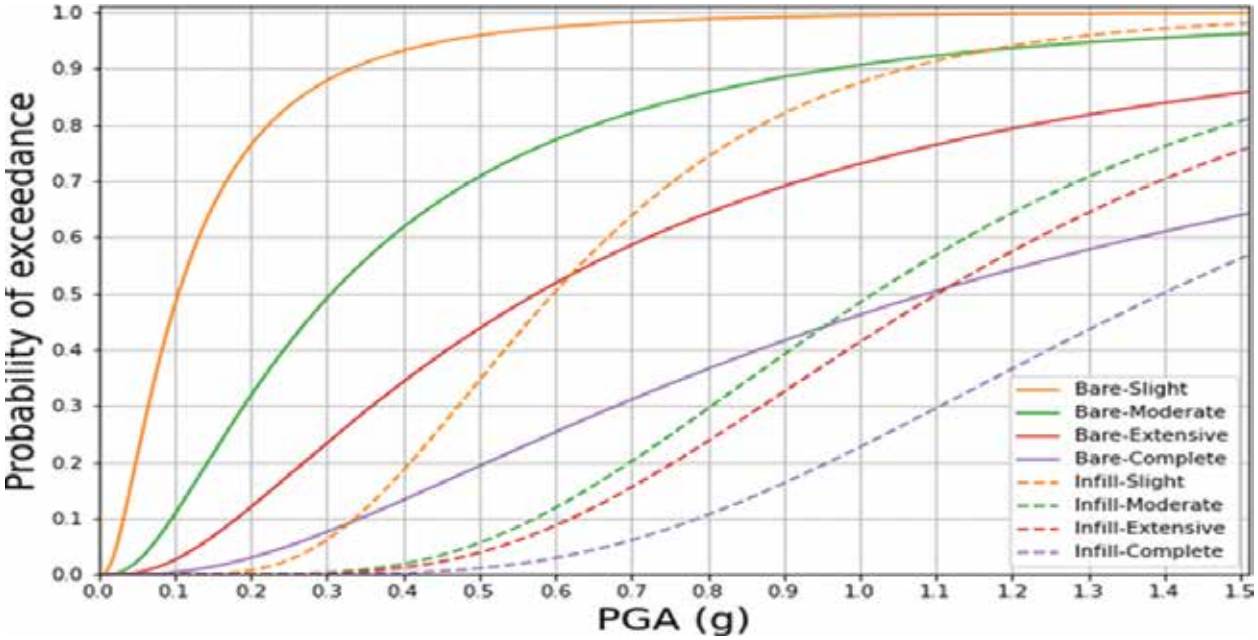

Figure 5: Analytical fragility curve

From the analytical fragility curve developed for bare and infill model, it was observed that at a seismic demand of 0.8g, the corresponding exceedance probabilities were respectively 98.81 %, 85.75%, 64.23% and 36.53% for slight, moderate, extensive and complete damage states in bare frame case. Similarly, for the infill case, the corresponding exceedance probabilities were 74.23%, 29.99%, 23.64% and 10.58% respectively for slight, moderate, extensive and complete damage states. For all the damage states, it was observed that the exceedance probabilities were high in case of bare frame model. This depicted that the bare frame was more vulnerable to a seismic event compared to infill frame.

4. Conclusions

In low-rise RC frame buildings in Nepal, masonry infills are most typical. It is also customary to disregard its impact during a seismic shaking. The effect of the infill masonry on the structural performance of low-rise RC frame was examined in this study. Two scenarios, bare and infill, were set, for the model. Roof displacement was considered as the global parameter in the analysis. At first, modal analysis was done for the bare frame model in order to validate the OpenSees model. Fragility curves were also developed for the case of bare and infill. The study revealed that, the inclusion of the infills were associated with the drastic reduction of the roof displacement of the RC frame. The results from the analytical fragility function revealed that, bare frame structure was more fragile or vulnerable to an earthquake event compared to the infill structure. At 0.8g, the damage state fragility for the bare frame case was 98.81 %, 85.75%, 64.23% and 36.53% for slight, moderate, extensive and complete damage states. Similarly, for the infill case, the corresponding exceedance probabilities were 74.23%, 29.99%, 23.64% and 10.58% respectively for slight, moderate, extensive and complete damage states at a PGA of 0.8g. Hence, the inclusion of the infill effect is thus recommended during the analysis and design of the low-rise RC frame in context of Nepal. For the further consideration of this work, soil-structure interaction can be considered. The infill effect, taking into account the openings can be considered for further expansion of this research work. The combined effect of in-plane as well as out-of-plane effect of the infill masonry could be the further aspect of this study.

Declaration of Competing Interest

The authors declare that they have no known competing financial interests or personal relationships that could have appeared to influence the work reported in this paper.

References

Adhikari, R., Rupakhety, R., Giri, P., Baruwal, R., Subedi, R., Gautam, R., & Gautam, D. (2022). Seismic Fragility Analysis of Low-Rise RC Buildings with Brick Infills in High Seismic Region with Alluvial Deposits. *Buildings*, *12*(1). https://doi.org/10.3390/buildings12010072

Ancheta, T., Darragh, R., Stewart, J., Seyhan, E., Silva, W., Chiou, B., Wooddell, K., Graves, R., Kottke, A., Boore, D., Kishida, T., & Donahue, J. (2013). *PEER NGA-West2 Database*, *Technical Report PEER 2013/03. May 2013.*

Andre Filipe Furtado,Hugo rodrigues,H.Varum, A. C. (2014). Assessment and strengthening strategies of existing RC buildings with potential soft-storey response. *9th International Masonry Conference*, *July*, 1–9.

Asteris, P. G., Cavaleri, L., Di Trapani, F., & Tsaris, A. K. (2017). Numerical modelling of out-of-plane response of infilled frames: State of the art and future challenges for the equivalent strut macromodels. *Engineering Structures*, *132*, 110–122. https://doi.org/10.1016/j.engstruct.2016.10.012

Asteris, Panagiotis G., Cavaleri, L., Di Trapani, F., & Sarhosis, V. (2015). A macro-modelling approach for the analysis of infilled frame structures considering the effects of openings and vertical loads. *Structure and Infrastructure Engineering*, *12*(5), 551–566. https://doi.org/10.1080/15732479.2015.1030761

Asteris, Panagiotis G., Tsaris, A. K., Cavaleri, L., Repapis, C. C., Papalou, A., Di Trapani, F., & Karypidis, D. F. (2016). Prediction of the fundamental period of infilled rc frame structures using artificial neural networks. *Computational Intelligence and Neuroscience*, *2016*. https://doi.org/10.1155/2016/5104907

Barbosa, A. R., Fahnestock, L. A., Fick, D. R., Gautam, D., Soti, R., Wood, R., Moaveni, B., Stavridis, A., Olsen, M. J., & Rodrigues, H. (2017). Performance of Medium-to-High Rise Reinforced Concrete Frame Buildings with Masonry Infill in the 2015 Gorkha, Nepal, Earthquake. *Earthquake Spectra*, *33*(Special issue 1), S197–S218. https://doi.org/10.1193/051017EQS087M

Carreo, R., Asce, S. M., Lotfizadeh, K. H., & Asce, S. M. (2020). *Material Model Parameters for the Giuffrè-Menegotto-Pinto Uniaxial Steel Stress-Strain Model*. *146*(2), 1–21. https://doi.org/10.1061/(ASCE)ST.1943-541X.0002505

Chopra, A. K. (2001). Dynamics of structures: Theory and applications to earthquake engineering, 2nd edition. In *Earthquake Spectra* (Vol. 17, Issue 3, p. 549). https://doi.org/10.1193/1.1586188

Dolšek, M., & Fajfar, P. (2008). The effect of masonry infills on the seismic response of a four-storey reinforced concrete frame - a deterministic assessment. *Engineering Structures*, *30*(7), 1991–2001. https://doi.org/10.1016/j.engstruct.2008.01.001

Fardis, T. B. P. M. N. (1996). *Seismic Response of Infilled RC Frames Structures*. 11th World Conference on Earthquake Engineering.

Federal Emergency Management Authority. (2003). California USA.

Fikri, R., & Ingham, J. (2022). Seismic response and aftershock fragility curves for Non-ductile Mid-rise buildings comprised of reinforced concrete frame with masonry infill. *Structures*, *45*(October), 1688–1700. https://doi.org/10.1016/j.istruc.2022.09.108

Frank McKenna, Gregory L Fenves, M. H. S. (2000). *Open System For Earthquake Engineering Simulation(OpenSees)*.

Furtado, A., Rodrigues, H., & Arêde, A. (2015). Modelling of masonry infill walls participation in the seismic behaviour of RC buildings using OpenSees. *International Journal of Advanced Structural Engineering*, *7*(2), 117–127. https://doi.org/10.1007/s40091-015-0086-5

Furtado, A., Rodrigues, H., Arêde, A., & Varum, H. (2015). Influence of the in Plane and Out-of-Plane Masonry Infill Walls' Interaction in the Structural Response of RC Buildings. *Procedia Engineering*, *114*, 722–729. https://doi.org/10.1016/j.proeng.2015.08.016

Kose, M. M. (2009). Parameters affecting the fundamental period of RC buildings with infill walls. *Engineering Structures*, *31*(1), 93–102. https://doi.org/10.1016/j.engstruct.2008.07.017

Lagomarsino, S., & Giovinazzi, S. (2006). Macroseismic and mechanical models for the vulnerability and damage assessment of current buildings. *Bulletin of Earthquake Engineering*, *4*(4), 415–443. https://doi.org/10.1007/s10518-006-9024-z

Mander, J. B., Priestley, M. J. N., & Park, R. (1989). Theorotical Stress-Strain Model For Confined Concrete. *J. Struct. Eng*, *114*(8), 1804–1826.

Mohammad Noh, N., Liberatore, L., Mollaioli, F., & Tesfamariam, S. (2017). Modelling of masonry infilled RC frames subjected to cyclic loads: State of the art review and modelling with OpenSees. *Engineering Structures*, *150*, 599–621. https://doi.org/10.1016/j.engstruct.2017.07.002

Neuenhofer, A., & Filippou, F. C. (1997). Evaluation of Nonlinear Frame Finite-Element Models. *Journal of Structural Engineering*, *123*(7), 958–966. https://doi.org/10.1061/(asce)0733-9445(1997)123:7(958)

PEER. (2005). *Strong Motion Database*. https://ngawest2.berkeley.edu/

Pujol, S., & Fick, D. (2010). The test of a full-scale three-story RC structure with masonry infill walls. *Engineering Structures*, *32*(10), 3112–3121. https://doi.org/10.1016/j.engstruct.2010.05.030

Rodrigues, H., Varum, H., & Costa, A. (2010). Simplified macro-model for infill masonry panels. *Journal of Earthquake Engineering*, *14*(3), 390–416. https://doi.org/10.1080/13632460903086044

Scott, M. H. (2007). Numerical Integration Options for the Force-Based Beam-Column Element in OpenSees. *Journal of Intelligent Material Systems and Structures*, *18*(19), 1111-1120.

Shan, S., Li, S., Xu, S., & Xie, L. (2016). Experimental study on the progressive collapse performance of RC frames with infill walls. *Engineering Structures*, *111*, 80–92. https://doi.org/10.1016/j.engstruct.2015.12.010

Teguh, M. (2017). Experimental Evaluation of Masonry Infill Walls of RC Frame Buildings Subjected to Cyclic Loads. *Procedia Engineering*, *171*, 191–200. https://doi.org/10.1016/j.proeng.2017.01.326

Uprety, R., & Suwal, R. (2023). Bidirectional effect of earthquake on low-rise RC frames with and without the consideration of In-plane effect of unreinforced masonry infill. *Structures*, *47*(November 2022), 648–664. https://doi.org/10.1016/j.istruc.2022.11.099

Varum, H. S. A. (2003). Seimic assessment, strengthening and repair of existing buildings. *PhD Thesis*, *Department of Civil Engineeinng*, *University of Averio*, *Portugal*, 1–508.